PAMM

WILEY-VCH

PAMM Proceedings in Applied Mathematics and Mechanics

RESEARCH ARTICLE OPEN ACCESS

Simulating Brittle Fracture With a Robust Hybrid Explicit–Implicit Solver for Staggered Phase-Field Problems

Seyed Farhad Hosseini | Mahan Gorji | Roman Sartorti | Lars Radtke | Alexander Düster

Numerical Structural Analysis with Application in Ship Technology (M-10), Hamburg, Germany

Correspondence: Seyed Farhad Hosseini (farhad.hosseini@tuhh.de)

Received: 8 May 2024 | **Revised:** 13 November 2024 | **Accepted:** 26 November 2024

Funding: This research was supported by Alexander von Humboldt Foundation. Furthermore, the authors gratefully acknowledge the support provided by the DFG (Deutsche Forschungsgemeinschaft) under the grant number DU 405/17-2 with the project number 168 448085183 and the grant number DU 405/21-1 with the project number 505137962.

Abstract

In this work, the robustness of phase-field fracture simulations is increased by introducing a new hybrid approach to take advantages of both explicit and implicit solvers. Switching to an explicit solver at critical load cases enables us to define a threshold on the maximum number of staggered iterations per load step. Having this threshold would be very useful in complicated FCM problems since we cannot wait for a full convergence of the implicit solver at critical load steps. With the new hybrid method, the problem is implicit as long as the implicit solver can converge within a specified threshold; otherwise, the failed load step will be solved robustly using an explicit approach. The method can resolve the highly nonlinear part of the global load–displacement curve. The superiority of the approach is shown in different benchmark examples.

1 | Introduction

The phase-field modeling of brittle fracture addresses a coupling between the elastic field and the crack phase-field. In phase-field modeling, a crack is not a discrete and discontinuous feature but a smooth transition from fully cracked toward the intact area [1, 2]. This transition is defined by a length-scale parameter which must be greater than the size of a couple of elements at the critical region.

For predicting the crack initiation/propagation in complex geometries, the phase-field approach can be integrated to the finite cell method (FCM). The basic idea of the FCM is to combine the existing physical domain with a fictitious domain in order to have an extended domain which is simple to mesh [3, 4]. On the other hand, this simple mesh generation makes the integration of broken elements/cells more difficult. In the FCM, the physical/implicit geometry is immersed in a simple structured mesh and special integration methods like space-tree [5, 6] or moment fitting [7, 8] should be employed. In space-tree methods, broken cells are subdivided into smaller sub-cells to increase the accuracy of integration, while moment-fitting methods generate cell-specific quadrature points and weights. The combination of the phase-field approach with the FCM has been already addressed in previous works like [9, 10].

The coupled phase-field problems can be solved either monotonically [11, 12] or by using the staggered [13, 14] approaches. In the monolithic approach, the system of coupled differential equations is solved simultaneously, while in the staggered schemes, displacement, and phase-fields are solved separately together with exchanging required data at each iteration. The monolithic approach has a high convergence rate but suffers from convergence issues, especially at highly nonlinear load steps. On the other hand, staggered approaches are robust and are easier to be implemented in existing software. Staggered approaches can also be divided into explicit staggered as well as implicit staggered ones [15]. In the explicit approach, there is no convergence check

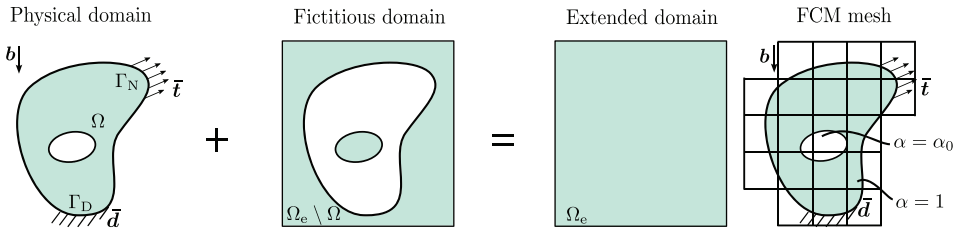

FIGURE 1 | Sketch of the idea behind the FCM. The physical domain is combined with a fictitious domain, such that the extended domain can be discretized using Cartesian meshes.

after each iteration, but very refined load steps are needed for fair accuracy. Therefore, the advantage of the implicit approach is the accuracy, but the advantage of the explicit approach is the robustness, it means that choosing between the implicit or explicit approach is choosing between accuracy and robustness.

In FCM problems, we cannot always afford the high number of iterations needed for the implicit solvers to converge. On the other hand, opting for a fully explicit scheme without previous knowledge of the level of refined load steps is also risky. In this paper, we introduce a solution to take advantage of both methods. According to the new method, a threshold is defined as the maximum number of staggered iterations. The solver is implicit as long as this threshold has not been reached; otherwise, the failed load step is divided into a set of refined explicit sub-load steps. With this hybrid method, we try to capture both the accuracy of the implicit approach and the robustness of the explicit approach.

The paper is organized as follows: Section 2 introduces the theoretical prerequisites. The proposed hybrid approach is explained in Section 3. In Section 4, two benchmark examples are provided to show the advantage of the proposed method. Finally, the paper is concluded in Section 5.

2 | Theoretical Backgrounds

2.1 | The Finite Cell Method

The concept of the FCM is shown in Figure 1. In FCM, a fictitious domain is added to the physical domain to have a simple-shape extended domain. This extended domain can be meshed easily. During the integration phase, the indicator function $\alpha(\boldsymbol{x})$ is used to distinguish between the physical and the fictitious domain integration points:

$$\alpha(\boldsymbol{x}) = \begin{cases} 1, & \boldsymbol{x} \in \Omega \\ \alpha_0, & \boldsymbol{x} \in \Omega_e \setminus \Omega \,, \end{cases} \tag{1}$$

α_0 is the stabilization parameter which is usually chosen to be a very small positive number to avoid ill-conditioning of the stiffness matrices. For linear elastic problems, the weak form for the extended domain is given by

$$\int_{\Omega_e} \alpha(\boldsymbol{x}) \delta\boldsymbol{\varepsilon} \cdot \boldsymbol{\sigma} \, \mathrm{d}\Omega = \int_{\Omega_e} \alpha(\boldsymbol{x}) \delta\boldsymbol{u} \cdot \boldsymbol{b} \, \mathrm{d}\Omega + \int_{\Gamma_N} \delta\boldsymbol{u} \cdot \bar{\boldsymbol{t}} \, \mathrm{d}\Gamma \,, \tag{2}$$

$\boldsymbol{\sigma}$ is the Cauchy stress, $\delta\boldsymbol{u}$ is the virtual displacement, $\boldsymbol{b}$ is the body force, $\delta\boldsymbol{\varepsilon}$ is the virtual strain and finally $\bar{\boldsymbol{t}}$ is the traction force. For further details, interested readers may refer to [3, 16, 17].

The complexity arises when it comes to the integration of the broken cells. There are various methods to tackle this challenge among them are the space-tree methods, the moment-fitting methods, and the nonnegative moment-fitting method. Space-tree methods are very robust but numerically expensive due to very large number of integration points needed [5]. In order to reduce the number of integration points, the moment-fitting can be employed, which creates a special case of the quadrature rule for each broken cell [8]. In the current work, we use the nonnegative moment fitting approach, which is an extended version of the standard moment fitting method [18, 19]. The nonnegative moment fitting approach forces the weights to be positive, which has a strong effect on the stability of the numerical integration.

2.2 | Phase-Field Fracture

The main concept of the phase-field approach is shown in Figure 2. The total potential energy of a cracked system is defined by adding the fracture surface energy $\mathcal{E}_s$ to the classical elastic energy $\mathcal{E}_{el}$ [10, 20]

$$\mathcal{E}(\boldsymbol{u}) = \underbrace{\int_{\Omega \setminus \Gamma_s} \Psi_e(\boldsymbol{\varepsilon}(\boldsymbol{u})) \, \mathrm{d}\Omega}_{\mathcal{E}_{el}(\boldsymbol{u})} + \underbrace{\int_{\Gamma_s} G_c \, \mathrm{d}\Gamma}_{\mathcal{E}_s} \,. \tag{3}$$

G_c is the material's fracture energy and Ψ_e denotes the strain energy density. According to the phase-field concept, a sharp crack is regularized through a smooth function $s(\boldsymbol{x}, t)$, therefore, Equation (3) can be rewritten as [21, 22]

$$\mathcal{E}(\boldsymbol{u}, s) = \underbrace{\int_{\Omega} g(s) \, \Psi_e(\boldsymbol{u}) \, \mathrm{d}\Omega}_{\mathcal{E}_{el}(\boldsymbol{u},s)} + \underbrace{\int_{\Omega} \frac{G_c}{c_w} \left(\frac{w(s)}{\ell} + \ell \, |\nabla s|^2 \right) \mathrm{d}\Omega}_{\mathcal{E}_s(s)} \,. \tag{4}$$

In this equation, $g(s)$ is the degradation function, $w(s)$ is the dissipation function and $\ell_0 \ll \mathrm{size}(\Omega)$ is the length-scale parameter. The length-scale parameter defines the intensity of regularization. In the current work, a quadratic degradation function, namely $g(s) = (1-s)^2 + \kappa$, is employed where $\kappa \ll 1$ is a stability parameter. Also we utilize an AT-2 model for the dissipation function, $w(s) = s^2$ and $c_w = 2$ [22].

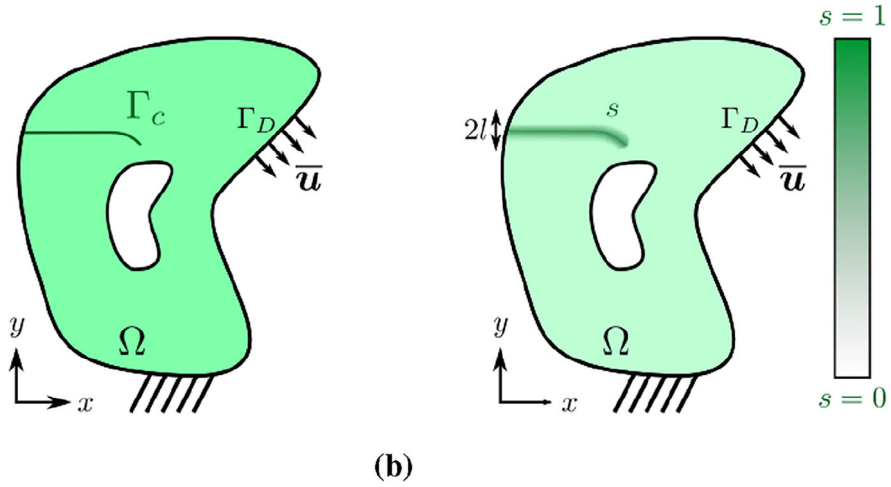

FIGURE 2 | Phase-field modeling approach. (a) Problem setup with sharp crack representation and (b) smooth crack representation by the phase-field s.

Deriving the weak form and then discretization are the very next steps to obtain the system of coupled equations. A history field is adopted to enforce the irreversibility [23]. Furthermore, a hybrid volumetric-deviatoric strain energy split is used to prevent crack formation due to compressive stresses [24].

In this work, this system of coupled equations is solved using the staggered approach. In contrast to the fully coupled monolithic approach, the staggered approach has the advantage of a better convergence at critical load steps as well as simplicity in implementation within already existing finite element (FE) software. The staggered approach can be implemented in both explicit and implicit manners, as shown in Figure 3. As can be inferred, the implicit approach is a very accurate method since it checks the convergence of each load step, but implicit solvers lack robustness at crack initiation/propagation load steps. On the other hand, the explicit approaches are very robust, but a very large number of load steps are needed for fair accuracy. In the next section, we introduce a hybrid method to gain the advantages of both solvers.

3 | Combined Implicit–Explicit Scheme

In phase-field simulations of brittle fracture, it is very common to face very strong nonlinearities. These nonlinearities have physical interpretations like sudden crack growth within the domain. At these highly nonlinear load steps, implicit solvers need a very large number of iterations to obtain convergence. In complex problems, such a high number of iterations is prohibitive. Also, due to the zigzag behavior of the residuals at critical load steps, a higher number of unconverged iterations does not necessarily mean higher accuracy.

In this work, we introduce a combined explicit–implicit approach to increase the robustness of FCM phase-field simulations. The concept of this hybrid method is shown in Figure 4. The approach is implicit as long as the maximum number of staggered iterations (MNoSI) is reached; otherwise, the implicit-failed load step is solved using a predefined set of explicit sub-load steps. The predefined number of explicit load steps is called the "number of local explicit load steps" or "number of local explicit load steps (NoLELS)" in Figure 4. Overall, the explicit solver can robustly bypass highly nonlinear load steps that are difficult to solve implicitly. The superiority of the hybrid method will be discussed in two benchmark examples in the next section. In this work, the phase-field approach is integrated with the FCM within the framework of a finite cell code called `AdhoC++` [25].

4 | Benchmark Examples

Two benchmark examples are provided in this section to numerically investigate the proposed method. The effect of different model parameters is also discussed accordingly.

4.1 | Notched Plate With Hole (2D)

The geometry and material/simulation data of this example are shown in Figure 5 and Table 1. Two small pinholes are the places where mechanical boundary conditions are applied: the plate is fixed at the lower pinhole and a displacement is applied at the top pinhole is loaded. The plate is fixed; as mentioned earlier, the mesh in the FCM is not boundary conforming; therefore, the middle hole in this example is taken into account only during the integration step.

As it can be seen in Figure 5, multilevel hp refinement is employed to refine the predicted crack path area. It should be pointed out that due to the simplicity of elements in FCM, multilevel hp refinement can be applied to almost all FCM examples if needed. Also, the preexisting crack is defined using Dirichlet boundary conditions. For better understanding, two holes at the load introduction points are shown in Figure 5, but in reality, loads, and boundary conditions are applied directly on bounded nodes without further considerations. The fully propagated crack path is also shown in Figure 5 which is consistent with the literature [26].

The effect of different NoLELS and MNoSI values are shown in Figures 6 and 7. In Figure 6, the value of NoLELS is fixed to 100. This figure shows that combined explicit–implicit cases follow

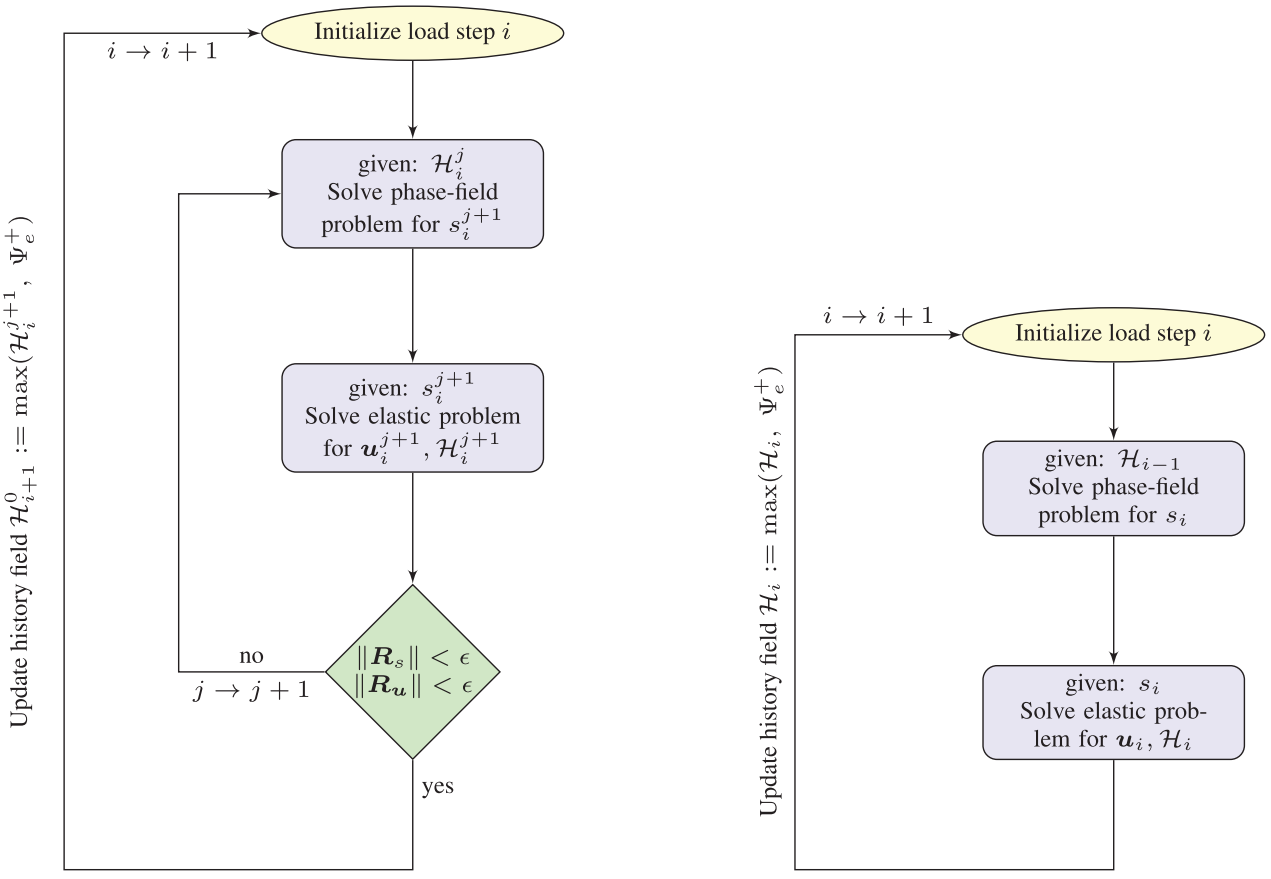

(a) Implicit staggered approach **(b)** Explicit staggered approach

FIGURE 3 | Flowcharts of the (a) implicit and (b) explicit staggered phase-field approaches.

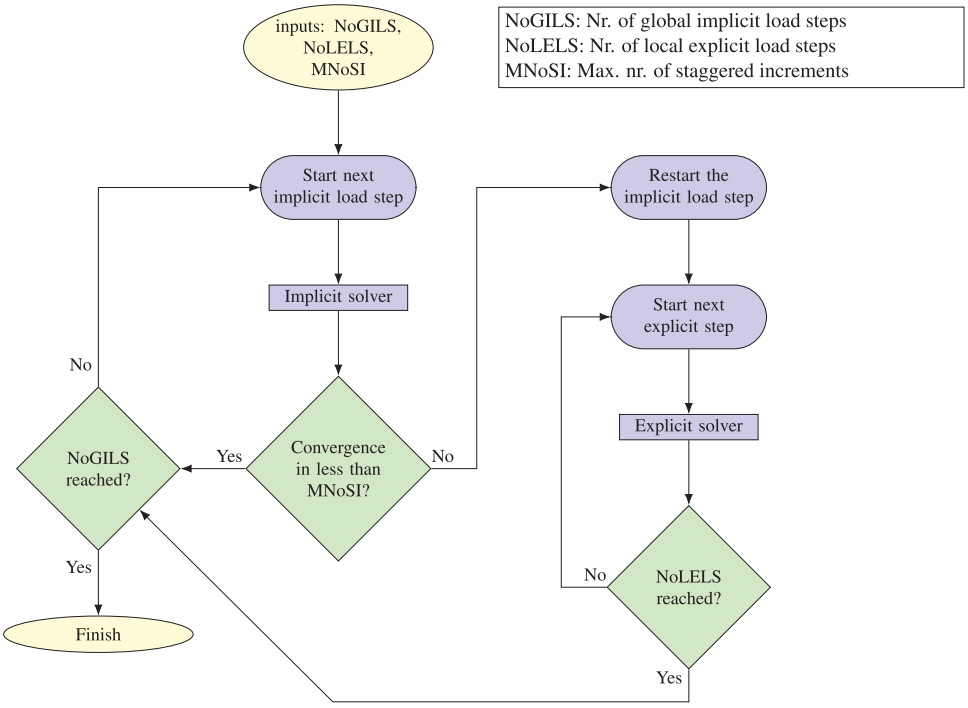

FIGURE 4 | Flowchart of the combined explicit–implicit approach.

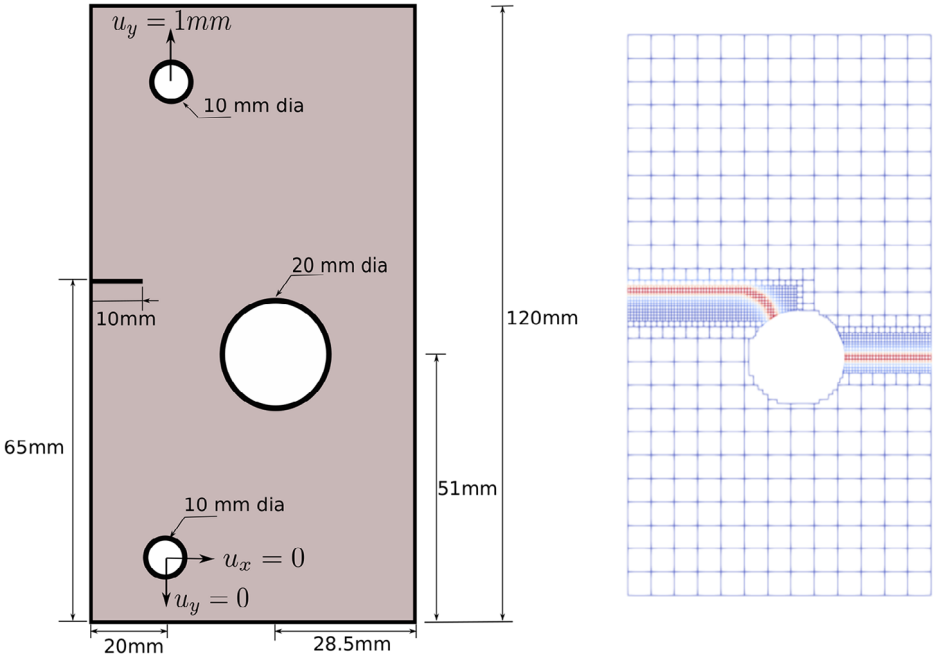

FIGURE 5 | Notched plate with hole: geometry and mesh (including fully propagated crack path).

TABLE 1 | Material/solver input parameters for the first benchmark example.

E	5.982 kN/mm^2
υ	0.22
G_c	2.28 N/mm
l_0	1.25 mm
κ	10^{-6}
α_{FCM}	10^{-8}
Convergence tolerance	10^{-5}
Space-tree subdivision depth within non-negative moment fitting (NNMF)	5
Load step	0.01 mm
Cell type	Four-node linear rectangular cell
Number of global implicit load steps (NoGILS)	100
Multilevel h-refinement level at critical areas	3

Note: Number of global implicit load steps.

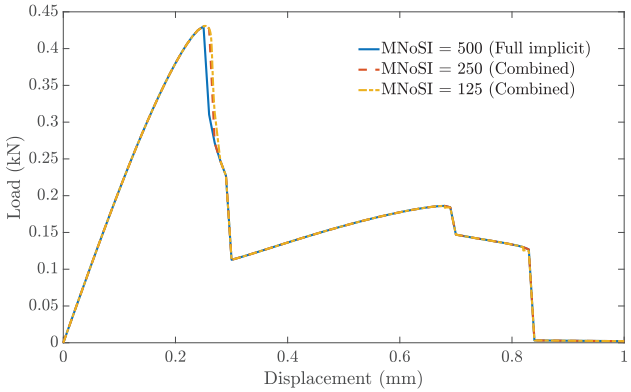

FIGURE 6 | Notched plate with hole: load–displacement curves for different MNoSI values (NoLELS = 100).

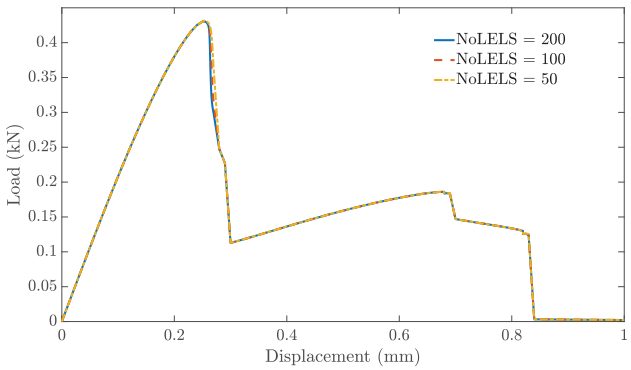

FIGURE 7 | Notched plate with hole: load–displacement curves for different NoLELS values (MNoSI = 125).

the full implicit curve quite well. It means that without existing information about the maximum number of staggered iterations for full implicit convergence, a hybrid method with insufficient number of staggered iterations makes the solver more robust. In Figure 7, the value of MNoSI is fixed to 125. This figure shows that by increasing NoLELS, the resulting curve follows the full-implicit curve more closely. In fact, by having a higher number of explicit sub-load steps, it is more likely to have convergence of the implicit approach in the subsequent load steps. Overall, it should be mentioned that all load–displacement curves are almost similar and using the hybrid formulation, no preexisting information on the number staggered information for a full-converged situation is needed and, on the other hand, we have not continued with an unconverged load step. It should be again

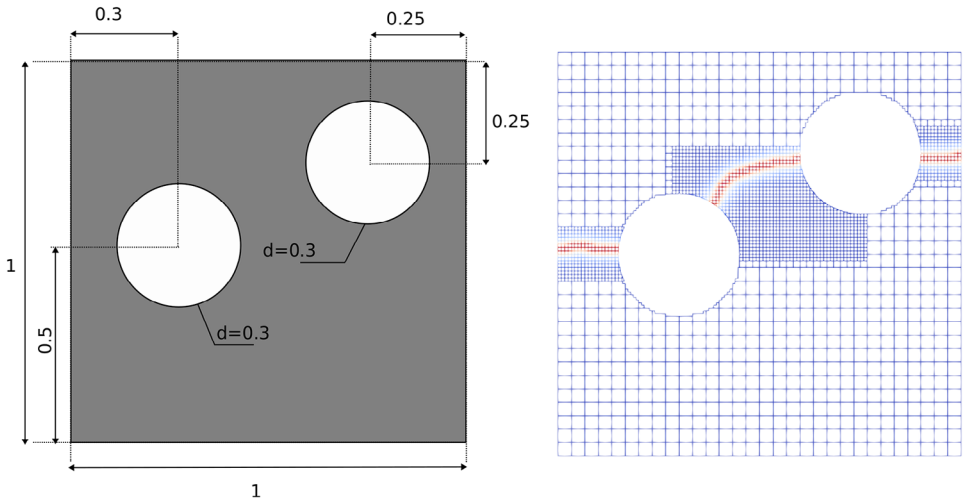

FIGURE 8 | Plate with two holes: geometry and mesh (including fully propagated crack path).

TABLE 2 | Material/solver input parameters for the second benchmark example.

E	210e3 MPa
υ	0.3
G_c	2.7 N/mm
l_0	0.0166 mm
κ	10^{-6}
α_{FCM}	10^{-6}
Convergence tolerance	10^{-5}
Space-tree subdivision depth within NNMF	6
Load step	0.0001 mm
Cell type	Four-node linear rectangular cell
Number of global implicit load steps (NoGILS)	70
Multilevel h-refinement level at critical areas	2

pointed out that in all cases, we have a very robust approach with almost similar load–displacement results in reasonable and predictable simulation time.

4.2 | Plate With Two Holes

The second benchmark example is a 2D square with two circular holes. Figure 8 demonstrates the geometry and meshing of this example. Material/solver input parameters of this example are provided in Table 2. The body is fixed at the bottom and loaded on the top.

In this example, the NoLELS value is fixed to 100, and the load–displacement results are provided for three MNoSI values. The load–displacement results are shown in Figure 9.

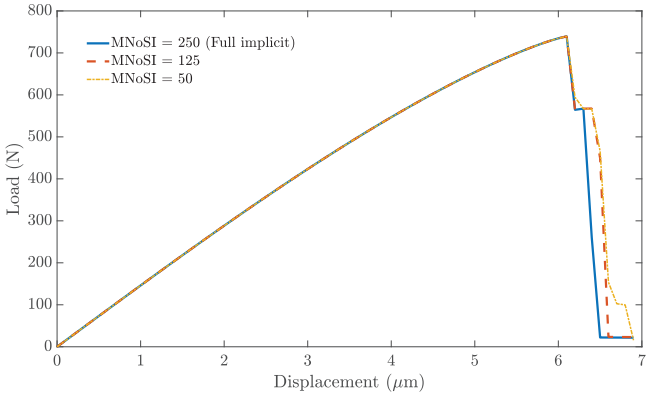

FIGURE 9 | Plate with two holes: load–displacement curves for different MNoSI values (NoLELS = 100).

The results suggest that in the hybrid cases, there would be a delay in sharp drops which can be controlled by refining the number of global load steps. However, like the first example, hybrid cases follow the accurate implicit case quite well and few differences can be compensated in the subsequent steps since the solver always tries to first solve the subsequent load steps implicitly.

5 | Conclusion

A hybrid explicit–implicit approach was introduced in this work to increase the robustness of solving FCM phase-field fracture problems. It was shown that the method successfully takes care of failed implicit load steps at critical crack initiation/propagation steps. The effect of different parameters like the maximum number of staggered iterations and/or the number of local explicit load steps was investigated and discussed. The results of two benchmark examples suggested that the load–displacement results obtained from the hybrid cases closely follow those of fully-converged implicit cases. In future, the method can be combined with the acceleration techniques to increase not only the robustness but also the speed of the analyses.

Acknowledgments

This research was supported by Alexander von Humboldt Foundation. Furthermore, the authors gratefully acknowledge the support provided by the DFG (Deutsche Forschungsgemeinschaft) under the grant number DU 405/17-2 with the project number 448085183 and the grant number DU 405/21-1 with the project number 505137962.

Open access funding enabled and organized by Projekt DEAL.

References

1. B. Bourdin, G. Francfort, and J.-J. Marigo, "Numerical Experiments in Revisited Brittle Fracture," *Journal of the Mechanics and Physics of Solids* 48, no. 4 (2000): 797–826.

2. P. Li, W. Li, B. Li, et al., "A Review on Phase Field Models for Fracture and Fatigue," *Engineering Fracture Mechanics* 289 (2023): 109419.

3. J. Parvizian, A. Düster, and E. Rank, "Finite Cell Method," *Computational Mechanics* 41 (2007): 121–133.

4. A. Düster, E. Rank, and B. Szabó, "The *p*-Version of the Finite Element and Finite Cell Methods," in *Encyclopedia of Computational Mechanics Second Edition*, eds. E. Stein, R. Borst, and T. J. R. Hughes (John Wiley & Sons, Ltd, 2017), 1–35.

5. A. Abedian, J. Parvizian, A. Düster, H. Khademyzadeh, and E. Rank, "Performance of Different Integration Schemes in Facing Discontinuities in the Finite Cell Method," *International Journal of Computational Methods* 10 (2013): 1350002.

6. L. Kudela, N. Zander, S. Kollmannsberger, and E. Rank, "Smart Octrees: Accurately Integrating Discontinuous Functions in 3D," *Computer Methods in Applied Mechanics and Engineering* 306 (2016): 406–426.

7. B. Müller, F. Kummer, and M. Oberlack, "Highly Accurate Surface and Volume Integration on Implicit Domains by Means of Moment-Fitting," *International Journal for Numerical Methods in Engineering* 96, no. 8 (2013): 512–528.

8. M. Joulaian, S. Hubrich, and A. Düster, "Numerical Integration of Discontinuities on Arbitrary Domains Based on Moment Fitting," *Computational Mechanics* 57 (2016): 979–999.

9. L. Hug, S. Kollmannsberger, Z. Yosibash, and E. Rank, "A 3D Benchmark Problem for Crack Propagation in Brittle Fracture," *Computer Methods in Applied Mechanics and Engineering* 364 (2020): 112905.

10. S. Nagaraja, M. Elhaddad, M. Ambati, S. Kollmannsberger, L. De Lorenzis, and E. Rank, "Phase-Field Modeling of Brittle Fracture With Multi-Level hp-FEM and the Finite Cell Method," *Computational Mechanics* 63 (2019): 1283–1300.

11. R. Bharali, S. Goswami, C. Anitescu, and T. Rabczuk, "A Robust Monolithic Solver for Phase-Field Fracture Integrated With Fracture Energy Based Arc-Length Method and Under-Relaxation," *Computer Methods in Applied Mechanics and Engineering* 394 (2022): 114927.

12. O. Lampron, D. Therriault, and M. Lévesque, "An Efficient and Robust Monolithic Approach to Phase-Field Quasi-Static Brittle Fracture Using a Modified Newton Method," *Computer Methods in Applied Mechanics and Engineering* 386 (2021): 114091.

13. C. Luo, "Fast Staggered Schemes for the Phase-Field Model of Brittle Fracture Based on the Fixed-Stress Concept," *Computer Methods in Applied Mechanics and Engineering* 404 (2023): 115787.

14. M. Kirkesæther Brun, T. Wick, I. Berre, J. M. Nordbotten, and F. A. Radu, "An Iterative Staggered Scheme for Phase Field Brittle Fracture Propagation With Stabilizing Parameters," *Computer Methods in Applied Mechanics and Engineering* 361 (2020): 112752.

15. Y. Lu, T. Helfer, B. Bary, and O. Fandeur, "An Efficient and Robust Staggered Algorithm Applied to the Quasi-Static Description of Brittle Fracture by a Phase-Field Approach," *Computer Methods in Applied Mechanics and Engineering* 370 (2020): 113218.

16. A. Düster, J. Parvizian, Z. Jun Yang, and E. Rank, "The Finite Cell Method for Three-Dimensional Problems of Solid Mechanics," *Computer Methods in Applied Mechanics and Engineering* 197 (2008): 3768–3782.

17. D. Schillinger, M. Ruess, N. Zander, Y. Bazilevs, A. Düster, and E. Rank, "Small and Large Deformation Analysis With the p- and B-Spline Versions of the Finite Cell Method," 50 (2012): 445–478.

18. G. Legrain, "Non-Negative Moment Fitting Quadrature Rules for Fictitious Domain Methods," *Computers & Mathematics with Applications* 99 (2021): 270–291.

19. W. Garhuom and A. Düster, "Non-Negative Moment Fitting Quadrature for Cut Finite Elements and Cells Undergoing Large Deformations," *Computational Mechanics* 70 (2022): 1059–1081.

20. G. A. Francfort and J.-J. Marigo, "Revisiting Brittle Fracture as an Energy Minimization Problem," *Journal of the Mechanics and Physics of Solids* 46, no. 8 (1998): 1319–1342.

21. B. Bourdin, G. Francfort, and J. J. Marigo, "The Variational Approach to Fracture," *Journal of Elasticity* 91, no. 4 (2008): 5–148.

22. L. De Lorenzis and T. Gerasimov, *Numerical Implementation of Phase-Field Models of Brittle Fracture* eds. L. De Lorenzis and A. Düster (Cham: Springer International Publishing, 2020), 75–101.

23. C. Miehe, F. Welschinger, and M. Hofacker, "Thermodynamically Consistent Phase-Field Models of Fracture: Variational Principles and Multi-Field FE Implementations," *International Journal for Numerical Methods in Engineering* 83, no. 10 (2010): 1273–1311.

24. M. Ambati, T. Gerasimov, and L. De Lorenzis, "A Review on Phase-Field Models of Brittle Fracture and a New Fast Hybrid Formulation," *Computational Mechanics* 55 (2015): 383–405.

25. A. Düster, H. Bröker, H. Heidkamp, et al., *Adhoc 4–User's Guide* (Munich: Technische Universität München, 2004).

26. T. Gerasimov and L. De Lorenzis, "A Line Search Assisted Monolithic Approach for Phase-Field Computing of Brittle Fracture," *Computer Methods in Applied Mechanics and Engineering* 312 (2016): 276–303.